

THE THREE-DIMENSIONAL STRUCTURE OF HOMOSERINE DEHYDROGENASE FROM MYCOBACTERIUM TUBERCULOSIS: AN *IN SILICO* STUDY

Bhawana Singh¹ and *Bhavya Jha²

¹Department of Zoology, RKD College, Patliputra University, Patna- 800020, Bihar, India

²Department of Zoology, Ganga Devi Mahila Mahavidyalaya, Patliputra University, Patna- 800020, Bihar, India

*Author for Correspondence: jha.bhavya18@gmail.com

ABSTRACT

Tuberculosis (TB), despite comprehensive efforts to culminate it, continues to be a global health crisis. Persistent rise of resistance against approved drugs including the newest one-Bedaquiline, raise an alarming situation. It warrants exploration of newer targets indispensable for the bug. In this context, the enzymes of aspartate biosynthesis pathway, a central metabolic pathway, present attractive targets to combat the causative organism, *Mycobacterium tuberculosis* (*Mtb*). Homoserine dehydrogenase (HSD) a key enzyme in the aspartate pathway, catalyses the reversible conversion of L-aspartate β -semialdehyde to L-homoserine, using NAD(H) or NADP(H) as a coenzyme. This enzyme is important for *Mtb* growth and pathogenicity. We report *in silico* structural characterization of *Mtb*-HSD. The crystal structure of *Mtb*-HSD is not yet available; its three-dimensional structure is predicted using AlphaFold tool. Physicochemical and stereochemical parameters were analysed to determine the accuracy of the AlphaFold predicted model. Sequence analysis and modelled structure revealed *Mtb*-HSD as a monofunctional enzyme containing three domains i.e., NAD-binding domain, catalytic domain, and ACT domain. This study forms the basis for future research pertaining to delineation of the active site of the enzyme and its critical interactions to aid inhibitor design against this enzyme.

Keywords: Tuberculosis, *Mycobacterium tuberculosis*, Aspartate biosynthesis, Homoserine dehydrogenase, AlphaFold model

INTRODUCTION

Tuberculosis (TB) is one of the earliest known diseases which has been a persistent health and economic issue for people worldwide, especially in low- and middle-income nations. Even today, TB is one of the top thirteen leading causes of morbidity and mortality globally (Yelamanchi and Surolia, 2021) and also a second leading infectious killer after SARS-CoV-2 in year 2021 (Global Tuberculosis Report, 2022; Chitale *et al.*, 2022). Year 2021 – 2023 recorded an increasing trend of TB incidences, bringing TB incidence rate of 2023 to the level of 2018 (Global Tuberculosis Report, 2024).

Mycobacterium tuberculosis (*Mtb*), the pathogenic bacteria that causes TB, has evolved a resistance to the existing medications, leading to the emergence of drug-resistant strains that create a major barrier to the advancement of TB control strategies (Brouqui *et al.*, 2017). Bedaquiline, the drug which was approved for treatment of drug resistant TB in 2012, has itself witnessed remarkable resistance in last few years (Satapathy *et al.*, 2024). Consequently, there is a pressing need to discover novel drug targets. Recent researches have indicated various central carbon metabolic pathways that are crucial to *Mtb* survival and pathogenicity (Cole *et al.*, 1998; DeJesus *et al.*, 2017; Wellington and Hung, 2018). The enzymes in these metabolic pathways can be targeted for therapeutic intervention (Murima *et al.*, 2014). Moreover, essential amino acid biosynthetic enzymes are largely missing in humans and found only in plants, fungi and bacteria (Wellington, 2018; Berney and Berney-Meyer, 2017; Evans and Mizrahi 2015; Wellington *et al.*, 2017)

and hence, can serve as selective targets. *Mtb* synthesizes most of its amino acids (Berney *et al.*, 2015) which makes the enzymes of these biosynthesis pathways promising drug target(s). One such pathway is aspartate pathway, where aspartate is converted into several essential amino acids, including threonine, lysine, methionine, and isoleucine (Berney *et al.*, 2015, Pavelka Jr and Jacobs Jr, 1996).

At first, the enzyme aspartate kinase mediates the phosphorylation of aspartate to aspartyl phosphate which is further transformed into L-aspartate- β -semialdehyde by aspartate semialdehyde dehydrogenase (Figure 1). The second product L-aspartate- β -semialdehyde subsequently undergoes metabolism to yield either L-homoserine (L-HSE) or L-lysine. Homoserine dehydrogenase (HSD), EC 1.1.1.3, is a key enzyme in the aspartate metabolic pathway. This oxidoreductase enzyme catalyses critical branch point i.e. the reversible conversion of L-aspartate- β -semialdehyde to L-HSE which is the third step of the aspartate pathway (Figure 1). L-HSE act as the precursor of L-threonine, L-isoleucine, and L-methionine.

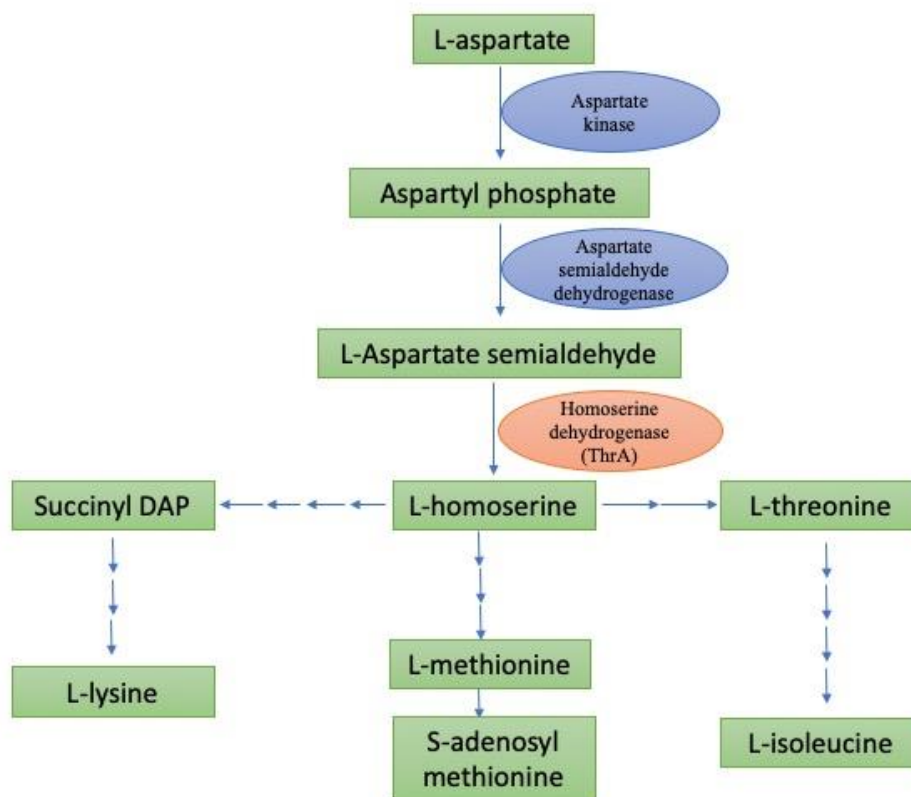


Figure 1: An overview of Aspartate degradation

Threonine and homoserine auxotrophs are bactericidal in *Mtb* (Hasenoehrl *et al.*, 2019) and the accumulation of homoserine in *Mtb* has been shown to be toxic (Yelamanchi and Surolia, 2021). Homoserine dehydrogenase is an established antifungal target (Han *et al.*, 2006; DeLaBarre *et al.*, 2000) and antibacterial target (Tang *et al.*, 2021). Collectively, these researches suggest that aspartate degradation pathway specifically HSD, one of the major regulatory enzymes of this pathway, may prove to be a promising anti-TB target.

Interestingly, this enzyme exists in two forms (Singh and Jha, 2024): monofunctional enzyme having HSD activity in yeast (Jacques *et al.*, 2001), some bacteria (Jacques *et al.*, 2001, Kim *et al.*, 2020) and archaea (Hayashi *et al.*, 2015) whereas bifunctional enzyme having HSD and additional aspartokinase (AK) activity in few bacteria (Ohshida *et al.*, 2018; Omori *et al.*, 1993) and plants (Weisemann and Matthews, 1993; Paris *et al.*, 2003). The activity of monofunctional enzyme may or may not be feedback-sensitive depending

upon its domain constitution. The activity of bifunctional enzyme has been reported to be sensitive to feedback inhibition by L-threonine (Navratna *et al.*, 2015).

The potential of *Mtb*-HSD as a drug target and the diversity observed in this enzyme among different organisms prompted us to delve further into its three-dimensional (3D) structure which provides the basis for delineation of its active site and corresponding enzyme-substrate interactions that can further be exploited for inhibitor design against it.

MATERIALS AND METHODS

Sequence analysis and physicochemical characterization

The amino acid sequence of *Mtb*-HSD was subjected to analysis by submitting the sequence in ExPASy ProtParam Server (Gasteiger *et al.*, 2005). This analysis provided a range of physicochemical characters of the submitted sequence including number of amino acids, molecular weight, theoretical pI, amino acid composition, number of negatively and positively charged amino acids, atomic composition, extinction coefficients, half-life, instability index, aliphatic index and Grand average of hydropathicity (GRAVY).

Secondary structure prediction

The secondary structure forms the base of protein folding. The secondary structure was predicted using SOPMA (Geourjon & Deleage, 1995) and PSIPred (McGuffin *et al.*, 2000). It provided with details of positions of helix, sheets, turns and other secondary structure elements in the amino acid sequence.

Mtb-HSD 3D structure prediction through AlphaFold AI

The amino acid sequence based predicted 3D structure of *Mtb*-HSD (AF-P9WPX1-F1) was available in AlphaFold Protein Structure Database (Varadi *et al.*, 2023; Jumper *et al.*, 2021) which hosts structures of over 200 million entries, providing broad coverage of UniProt, and freely accessible to the scientific community.

Structure validation and presentation

The 3D structure downloaded from AlphaFold Protein Structure database was subjected to analysis by employing SAVES v6.0 Structure validation server (<https://saves.mbi.ucla.edu/>); PROCHECK (Ramachandran plot, Chi1-Chi2 plots, G factors) (Laskowski *et al.*, 2006), ERRAT (Colovos & Yeates, 1993), and Verify3D (Lüthy *et al.*, 1992) programs. Structure presented in Figure 4 is made using PyMOL (Schrodinger, 2015).

RESULTS AND DISCUSSION

Physicochemical characterization of Mtb-HSD

Physicochemical characteristics of the enzyme are summarized in Table 1. Comprising 441 amino acids, the protein is slightly acidic with an isoelectric point (pI) in the acidic range. Its instability index, below 40, indicate a stable protein. An aliphatic index above 100 suggests high thermal stability. A positive Grand Average of Hydropathicity (GRAVY) value indicates polar nature of the protein.

Secondary Structure Prediction

A graphical representation of the secondary structure composition showing, percentage of different secondary structures and number of amino acids involved in forming a specific secondary structure is depicted in Figure 2A and 2B. Alpha helices are significantly more prevalent than beta sheets, while the proportion of random coils is comparable to that of alpha helix. These graphs are representation of the results obtained from SOPMA (Geourjon & Deleage, 1995) predicting three conformational states. Additionally, Figure 2C shows a PSIPred chart (McGuffin *et al.*, 2000) depicting the positions of strand, helices and coils along with prediction confidence. Notably, the confidence of prediction for majority of helices and sheets is significantly high.

Table 1: Physiochemical properties of *Mtb*-HSD

Number of amino acids		441	
Molecular weight		45552.74	
Theoretical pI		4.76	
Amino acid composition			
Amino acid	Abbreviation	Number	Percentage
Alanine	Ala (A)	70	15.9%
Arginine	Arg (R)	28	6.3%
Asparagine	Asn (N)	9	2.0%
Aspartic acid	Asp (D)	27	6.1%
Cysteine	Cys (C)	2	0.5%
Glutamine	Gln (Q)	7	1.6%
Glutamic acid	Glu (E)	30	6.8%
Glycine	Gly (G)	42	9.5%
Histidine	His (H)	5	1.1%
Isoleucine	Ile (I)	21	4.8%
Leucine	Leu (L)	38	8.6%
Lysine	Lys (K)	10	2.3%
Methionine	Met (M)	7	1.6%
Phenylalanine	Phe (F)	7	1.6%
Proline	Pro (P)	18	4.1%
Serine	Ser (S)	26	5.9%
Threonine	Thr (T)	26	5.9%
Tryptophan	Trp (W)	0	0.0%
Tyrosine	Tyr (Y)	11	2.5%
Valine	Val (V)	57	12.9%
Pyrrolysine	Pyl (O)	0	0.0%
Selenocysteine	Sec (U)	0	0.0%
Number of negatively charged residues	(Asp + Glu)	57	
Number of positively charged residues	(Arg + Lys)	38	
Extinction coefficients			
Extinction coefficient* ¹		16515	
Abs 0.1%* ²		0.363, assuming all pairs of Cys residues form cystines	
Extinction coefficient		16390	
Abs 0.1%		0.360, assuming all Cys residues are reduced	
Estimated half-life			
Mammalian reticulocytes, in vitro		30 hours	
Yeast, in vivo		>20 hours	
Escherichia coli, in vivo		>10 hours	
Instability index (II)		24.98	
Aliphatic index		105.53	
Grand average of hydropathicity (GRAVY)		0.242	

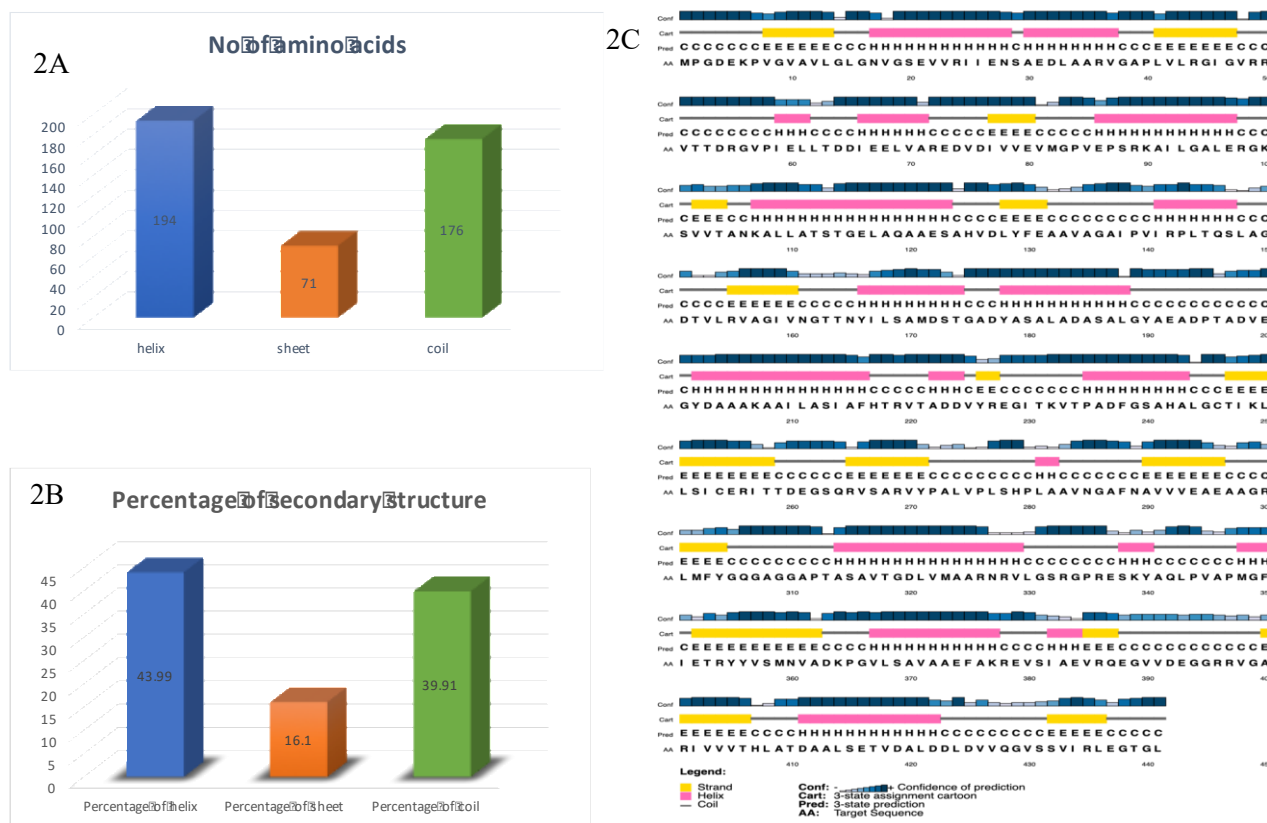


Figure 2: Secondary structure of *Mtb*-HSD. 2A. Number of amino acids involved in forming Helix, sheet and coil. 2B. Percentage of different secondary structures. 2C. Positions of different secondary structures are shown.

3D structure of *Mtb*-HSD

The 3D structure was predicted through the revolutionary AlphaFoldAI (Jumper et al., 2021), developed by Google DeepMind and European Bioinformatics Institute (EMBL-EBI). AlphaFold consistently achieves experimental-level accuracy, especially for proteins with homolog that have experimentally solved structures. A structure for UniProt entry P9WPX1, corresponding to *Mtb* HSD was available in the AlphaFold Protein Structure Database under the label "AF-P9WPX1-F1-model_v4.pdb" (Varadi *et al.*, 2023). The predicted structure was validated using SAVES v6.0 tool (<https://saves.mbi.ucla.edu/>). At first, Ramachandran plot analysis was performed employing PROCHECK (Laskowski *et al.*, 2012), which evaluates the stereochemical quality of the protein structure on a residue-by-residue basis. Notably, the analysis showed no Ramachandran outliers, indicating a good structure model (Figure 3). The overall quality G-factor was 0.1, signifying an acceptable model (PROCHECK values of the G-factor typically range from 0 to -0.5, with values near zero indicating good models). Since, there were no Ramachandran outliers in PROCHECK stereochemical analysis consequently no bad contacts or abnormal scores were evident for the main-chain or side-chain parameters. Further, ERRAT (Colovos & Yeates, 1993) which measures the quality of non-bonded atomic interactions was employed to assess the model quality. With a significantly high ERRAT score of 95.95, much ahead of the acceptable range (>50), the model can be categorized as a high-quality one. VERIFY 3D (Lüthy et al., 1992) analysis indicated a reasonably good sequence-to-structure agreement as 70.29% of the residues had an averaged 3D-1D score ≥ 0.1 , with only

0.03% residues showing a negative averaged score below -0.05, except one outlier with a score of -0.07. Overall, the model appears to be reasonably accurate.

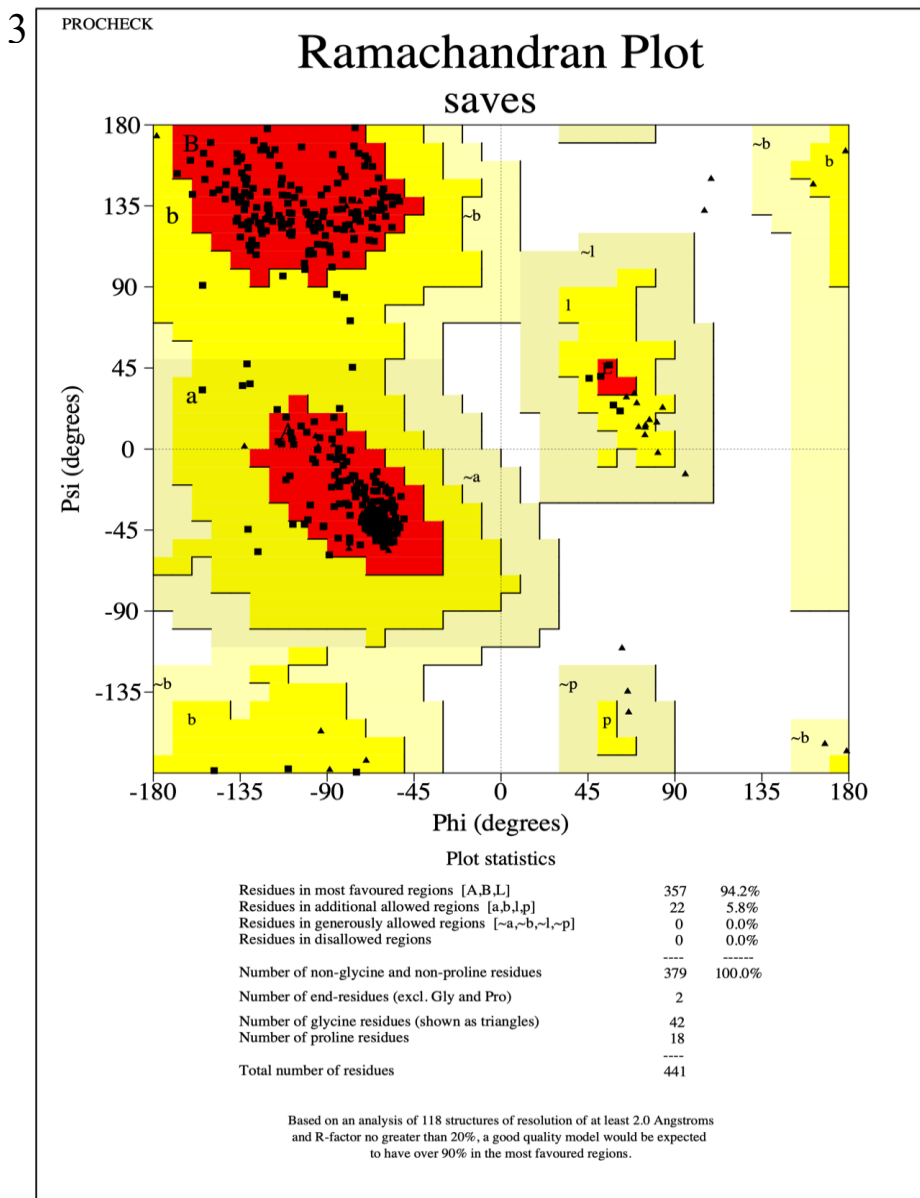


Figure 3: Ramachandran Plot of *Mtb*-HSD structure depicting 94.2% residues in most favoured regions and 5.8% residues in additional allowed regions. No outlier was observed.

Alike reported HSD structures, the three-dimensional structure of *Mtb* HSD also harbours a substrate binding as well as a nucleotide binding domain. Majority of monofunctional HSDs are reported to exist as a homodimer in solution. Nevertheless, the structures predicted through AlphaFold is of a single protein chain and hence, the structure of a monomer of *Mtb* HSD is reported here. However, when we provided an input of two protein sequences in AlphaMultimer (Evans et al., 2021), it built a homodimeric structure suggesting that this might be the case in solution.

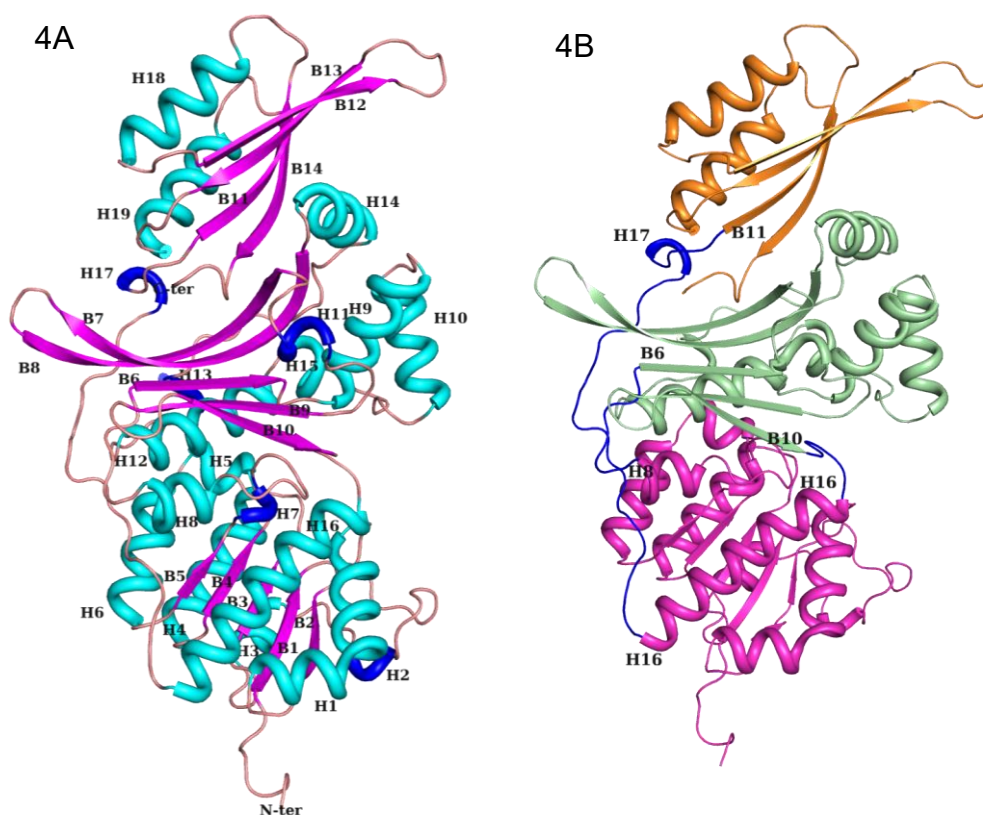


Figure 4: Three-dimensional structure of *Mtb*-HSD. 4A. Three-dimensional structure of *Mtb*-HSD is depicted in cartoon representation. Helices (cyan - α -type; blue - 3_{10} -type) and β -strands (pink) are numbered. Connecting loops are shown. 4B. Three domains of *Mtb*-HSD are shown in different colours: N-ter domain (pink), middle domain (green) and C-ter domain (orange). Connecting regions between the domains are shown in blue. Secondary structures, which share the domain connecting loops, are numbered.

Briefly, the 3D structure (Figure 4A) comprises 19 helices and 14 beta strands, interconnected by loops forming three distinct structural domains: An N-terminal domain, a middle domain and a C-terminal domain. The N-terminal domain – the functional NAD-binding domain is discontinuous (14-131 aa and 306-330). It comprises of five-stranded parallel beta sheet ($\beta 2 \uparrow \beta 1 \uparrow \beta 3 \uparrow \beta 4 \uparrow \beta 5 \uparrow$) sandwiched between helices H3, H4 and H6 on one side, and H1 and H16 on the other side (Figure 4A), H16 being the discontinuous segment. Additionally, H2, H5 and H7 flank the sandwiched sheet on the edges. The middle domain (139-322 aa) harbours a five-stranded anti-parallel beta sheet ($\beta 8 \uparrow \beta 7 \downarrow \beta 6 \uparrow \beta 9 \downarrow \beta 10 \uparrow$) cupped by helices H8, H12 and H13 on one side and H9, H10, H11, and H14 on the adjacent side. Two 3_{10} helices H15 and H17, form the rim of this cup. This domain houses the homoserine dehydrogenase catalytic site (Figure 4A). Finally, the smallest C-terminal domain (355- 437 aa) comprises of helices H18 and H19 situated on top of a four-stranded anti-parallel beta sheet ($\beta 12 \uparrow \beta 13 \downarrow \beta 11 \uparrow \beta 14 \downarrow$) and harbours the ACT regulatory domain (Figure 4A). The characteristic ferredoxin-like fold of ACT, a $\beta\alpha\beta\beta\alpha\beta$ unit in which four β -strands form an antiparallel β -sheet, while two α -helices are positioned together (Navratna *et al*, 2015) is evident in *Mtb* HSD structure ($\beta 11$ -H18- $\beta 12$ - $\beta 13$ -H19- $\beta 14$). A dimeric or tetrameric HSD attains

their state through its ACT domains forming a regulatory pocket. *Mtb*-HSD, based on the occurrence of ACT domain, is predicted as a feedback-sensitive member of the ACT domain-containing family proteins (Singh and Jha, 2024). The ACT domain appears in various contexts and is perceived to be a conserved regulatory binding fold. It is associated with a broad range of metabolic enzymes whose activity is regulated by amino acid concentrations. (Chipman and Shaanan, 2001), in this case by L-Threonine. The three domains are shown by different colours in Figure 4B. The discontinuous N-terminal domain is connected to the middle domain through a loop between H8 and $\beta 6$ and then again through a loop between $\beta 10$ and H16. The N-terminal domain is connected to the C-terminal ACT domain by a loop- $_{3-10}$ -helix-loop, the connecting region between H16 and B11, which transverse closely to the substrate binding region of middle domain, providing it an opportunity to regulate the catalytic activity. Studies have demonstrated that *Corynebacterium* HSD, an actinobacterial HSD, contains an ACT domain at the C-terminal end and can be allosterically inhibited by L-Threonine (Archer *et al.*, 1991). Since, *Mtb* is also an actinobacteria, possessing a HSD harbouring an ACT domain, it is likely to be allosterically inhibited by L-Thr. However, this needs to be substantiated by biochemical experiments. The physiochemical parameters categorize the protein as a stable one (Table 1), marking it favourable for overexpression and purification. Further studies exploring the nucleotide binding site and active site of the enzyme are warranted to exploit the potential of this very important enzyme as a target for anti-TB drugs.

CONCLUSION

Mtb-HSD is an essential enzyme for the growth and survival of *Mtb* and is notably absent in mammals, making it a promising selective target for anti-TB therapies. This study investigates the three-dimensional structure of *Mtb*-HSD using an in-silico approach, aiming to explore the different domains of this enzyme. It lays a groundwork for further delineation and characterization of the active site and the co-factor binding site of *Mtb*-HSD. Understanding the overall structure and active site structural features can guide the design of specific inhibitors, contributing to the development of targeted strategies for *Mtb* inhibition.

ACKNOWLEDGEMENTS

The authors acknowledge Dr. Deepak Kumar, Assistant Professor, Department of Zoology, University of Rajasthan for scientifically fruitful discussions.

REFERENCES

- Archer JAC, Solow-Cordero DE and Sinskey AJ (1991).** A C-terminal deletion in *Corynebacterium glutamicum* homoserine dehydrogenase abolishes allosteric inhibition by L-threonine. *Gene*, **107**(1), 53-59. [https://doi.org/10.1016/0378-1119\(91\)90296-N](https://doi.org/10.1016/0378-1119(91)90296-N)
- Berney M and Berney-Meyer L (2017).** Mycobacterium tuberculosis in the face of host-imposed nutrient limitation. *Tuberculosis and Tubercle bacillus*, 2nd edition, edited by Jacobs Jr. WR, McShane H, Mizrahi V and Orme IM (American Society for microbiology, Washington DC) 699-715. <https://doi.org/10.1128/9781555819569.ch33>
- Berney M, Berney-Meyer L, Wong KW, Chen B, Chen M, Kim J, Wang J, Harris D, Parkhill J, Chan J, Wang F. and Jacobs Jr. WR (2015).** Essential roles of methionine and S-adenosylmethionine in the autarkic lifestyle of Mycobacterium tuberculosis. *Proceedings of the National Academy of Sciences*, **112**(32), 10008-10013. <https://doi.org/10.1073/pnas.1513033112>
- Brouqui P, Quenard F and Drancourt M (2017).** Old antibiotics for emerging multidrug-resistant/extensively drug-resistant tuberculosis (MDR/XDR-TB). *International Journal of Antimicrobial Agents*, **49**(5), 554 – 557. <https://doi.org/10.1016/j.ijantimicag.2017.02.008>
- Chipman DM and Shaanan B (2001).** The ACT domain family. *Current opinion in structural biology*, **11**(6), 694-700. [https://doi.org/10.1016/S0959-440X\(01\)00272-X](https://doi.org/10.1016/S0959-440X(01)00272-X)
- Chitale P, Lemenze AD, Fogarty EC, Shah A, Grady C, Odom-Mabey AR, Johnson WE, Yang JH, Eren AM, Brosch R, Kumar P and Alland D (2022).** A comprehensive update to the Mycobacterium tuberculosis H37Rv reference genome. *Nature communications*, **13**(1), 7068. A comprehensive update to the Mycobacterium tuberculosis H37Rv reference genome. <https://doi.org/10.1038/s41467-022-34853-x>
- Cole S, Brosch R, Parkhill J, Garnier T, Churcher C, Harris D, Gordon SV, Eiglmeier K, Gas S, Barry Iii CE, Tekaia F.... and Barrell B G (1998).** Deciphering the biology of Mycobacterium tuberculosis from the complete genome sequence. *Nature*, **393**, 537 – 544 <https://doi.org/10.1038/31159>
- Colovos C and Yeates TO (1993).** Verification of protein structures: patterns of nonbonded atomic interactions. *Protein science*. **2**(9), 1511-9. <https://doi.org/10.1002/pro.5560020916>
- DeJesus MA, Gerrick ER, Xu W, Park SW, Long JE, Boutte CC, Rubin EJ, Schnappinger D, Ehrt S, Fortune SM and Sassetti CM (2017).** Comprehensive essentiality analysis of the Mycobacterium tuberculosis genome via saturating transposon mutagenesis. *MBio*, **8**(1), 10-1128. <https://doi.org/10.1128/mbio.02133-16>
- DeLaBarre B, Thompson PR, Wright GD and Berghuis AM (2000).** Crystal structures of homoserine dehydrogenase suggest a novel catalytic mechanism for oxidoreductases. *Nature structural biology*, **7**(3), 238-244. <https://doi.org/10.1038/73359>
- Evans JC and Mizrahi V (2015).** The application of tetracycline-regulated gene expression systems in the validation of novel drug targets in Mycobacterium tuberculosis. *Frontiers in Microbiology*, **6**, 812. <https://doi.org/10.3389/fmicb.2015.00812>
- Evans R, O'Neill M, Pritzel A, Antropova N, Senior A, Green T, Židek A, Bates R, Blackwell S, Yim J, Ronneberger O ...and Hassabis D (2021).** Protein complex prediction with AlphaFold-Multimer. *bioRxiv*, 2021-10. <https://doi.org/10.1101/2021.10.04.463034>
- Gasteiger E, Hoogland C, Gattiker A, Duvaud S, Wilkins MR, Appel RD and Bairoch, A (2005).** Protein Identification and Analysis Tools on the ExPASy Server In: *The Proteomics Protocols Handbook*, 1st edition, edited by Walker JM (Humana Press). 571-607. <https://doi.org/10.1385/1-59259-584-7:531>
- Geourjon C, and Deleage G (1995).** SOPMA: significant improvements in protein secondary structure prediction by consensus prediction from multiple alignments. *Bioinformatics*, **11**(6), 681-684. <https://doi.org/10.1093/bioinformatics/11.6.681>
- Global Tuberculosis Report 2022, WHO.** World Health Organization Geneva, Switzerland. <https://www.who.int/publications/i/item/9789240061729>

Global Tuberculosis Report 2024, WHO. World Health Organization Geneva, Switzerland.
<https://www.who.int/publications/i/item/9789240101531>

Han JY, Kwon YS, Yang DC, Jung YR and Choi YE (2006). Expression and RNA interference-induced silencing of the dammarediol synthase gene in *Panax ginseng*. *Plant and Cell Physiology*, **47**(12), 1653 – 62. <https://doi.org/10.1093/pcp/pcl032>

Hasenoehrl EJ, Rae Sajorda D, Berney-Meyer L, Johnson S, Tufariello JM, Fuhrer T, Cook GM, Jacobs Jr WR and Berney M (2019). Derailing the aspartate pathway of *Mycobacterium tuberculosis* to eradicate persistent infection. *Nature Communications*, **10**(1), 4215. <https://doi.org/10.1038/s41467-019-12224-3>

Hayashi J, Inoue S, Kim K, Yoneda K, Kawarabayasi Y, Ohshima T and Sakuraba H (2015). Crystal structures of a hyperthermophilic archaeal homoserine dehydrogenase suggest a novel cofactor binding mode for oxidoreductases. *Scientific Reports*, **5**(1), 11674. <https://doi.org/10.1038/srep11674>

Jacques SL, Nieman C, Bareich D, Broadhead G, Kinach R, Honek JF and Wright GD (2001). Characterization of yeast homoserine dehydrogenase, an antifungal target: the invariant histidine 309 is important for enzyme integrity. *Biochimica et Biophysica Acta (BBA) - Protein Structure and Molecular Enzymology*, **1544**(1 – 2), 28 – 41. [https://doi.org/10.1016/S0167-4838\(00\)00203-X](https://doi.org/10.1016/S0167-4838(00)00203-X)

Jumper J, Evans R, Pritzel A, Green T, Figurnov M, Ronneberger O, Tunyasuvunakool K, Bates R, Žídek A, Potapenko A, Bridgland A and Hassabis D (2021). Highly accurate protein structure prediction with AlphaFold. *Nature*, **596**, 583 – 89. <https://doi.org/10.1038/s41586-021-03819-2>

Kim DH, Nguyen QT, Ko GS and Yang JK (2020). Molecular and enzymatic features of homoserine dehydrogenase from *Bacillus subtilis*. *Journal of Microbiology and Biotechnology*, **30**(12), 1905-11. <https://doi.org/10.4014/jmb.2004.04060>

Laskowski RA, MacArthur MW and Thornton JM (2012). PROCHECK: validation of protein-structure coordinates In: *International Tables for Crystallography*, Volume F, 2nd edition, edited by Arnold E, Himmel DM and Rossmann MG (International Union of Crystallography, Chester, England), 684-687. <http://dx.doi.org/10.1107/97809553602060000882>

Lüthy R, Bowie JU and Eisenberg D (1992). Assessment of protein models with three-dimensional profiles. *Nature*, **356**(6364), 83 – 85. [https://doi.org/10.1016/s0076-6879\(97\)77022-8](https://doi.org/10.1016/s0076-6879(97)77022-8)

McGuffin LJ, Bryson K and Jones DT (2000). The PSIPRED protein structure prediction server. *Bioinformatics*, **16**(4), 404 – 405. <https://doi.org/10.1093/bioinformatics/16.4.404>

Murima P, McKinney JD and Pethe K (2014). Targeting bacterial central metabolism for drug development. *Chemical Biology*, **21**(11), 1423 – 32. <https://doi.org/10.1016/j.chembiol.2014.08.020>

Navratna V, Reddy G and Gopal B (2015). Structural basis for the catalytic mechanism of homoserine dehydrogenase. *Acta Crystallographica Section D: Biological Crystallography*, **71**(5), 1216 – 25. <https://doi.org/10.1107/s1399004715004617>

Ohshida T, Koba K, Hayashi J, Yoneda K, Ohmori T, Ohshima T and Sakuraba H (2018). A novel bifunctional aspartate kinase-homoserine dehydrogenase from the hyperthermophilic bacterium, *Thermotoga maritima*. *Bioscience, Biotechnology, and Biochemistry*, **82**(12), 2084 – 93. <https://doi.org/10.1080/09168451.2018.1511365>

Omori K, Imai Y, Suzuki S and Komatsubara S (1993). Nucleotide sequence of the *Serratia marcescens* threonine operon and analysis of the threonine operon mutations which alter feedback inhibition of both aspartokinase I and homoserine dehydrogenase I. *Journal of Bacteriology*, **175**(3), 785 – 794. <https://doi.org/10.1128/jb.175.3.785-794.1993>

Paris S, Viemon C, Curien G and Dumas R (2003). Mechanism of control of *Arabidopsis thaliana* aspartate kinase-homoserine dehydrogenase by threonine. *Journal of Biological Chemistry*, **278**(7), 5361 – 66. <https://doi.org/10.1074/jbc.m207379200>

- Pavelka MS Jr and Jacobs WR Jr (1996).** Biosynthesis of diaminopimelate, the precursor of lysine and a component of peptidoglycan, is an essential function of *Mycobacterium smegmatis*. *Journal of Bacteriology*, **178**(22), 6496 – 507. <https://doi.org/10.1128/jb.178.22.6496-6507.1996>
- Satapathy P, Itumalla R, Neyazi A, Taraki AMN, Khatib MN, Gaidhane S, Zahiruddin QS, Rustagi S and Neyazi M (2024).** Emerging bedaquiline resistance: a threat to the global fight against drug-resistant tuberculosis. *Journal of Biosafety and Biosecurity*, **6**(1), 13 – 15. <https://doi.org/10.1016/j.jobb.2024.01.001>
- Singh B and Jha B (2024).** Phylogeny of homoserine dehydrogenase. *CIBTech Journal of Zoology*, **13**, 124 – 130. <https://www.cibtech.org/J-Zoology/PUBLICATIONS/2024/CJZ-015-BHAVYA-PHYLOGENGY-DEHYDROGENASE.pdf>
- Schrodinger, L. L. C. (2015).** The PyMOL molecular graphics system. Version, 3.
- Tang W, Dong X, Meng J, Feng Y, Xie M, Xu H and Song P (2021).** Biochemical characterization and redesign of the coenzyme specificity of a novel monofunctional NAD⁺-dependent homoserine dehydrogenase from the human pathogen *Neisseria gonorrhoeae*. *Protein Expression and Purification*, **186**, 105909. <https://doi.org/10.1016/j.pep.2021.105909>
- Varadi M, Bertoni D, Magana P, Paramval U, Pidruchna I, Radhakrishnan M, Tsenkov M, Nair S, Mirdita M, Yeo J and Kovalevskiy O (2024).** AlphaFold Protein Structure Database in 2024: providing structure coverage for over 214 million protein sequences. *Nucleic Acids Research*, **52**(D1), D368 – D375. <https://doi.org/10.1093/nar/gkad1011>
- Weisemann JM and Matthews BF (1993).** Identification and expression of a cDNA from *Daucus carota* encoding a bifunctional aspartokinase-homoserine dehydrogenase. *Plant Molecular Biology*, **22**(2), 301 – 312. <https://doi.org/10.1007/bf00014937>
- Wellington S and Hung DT (2018).** The expanding diversity of *Mycobacterium tuberculosis* drug targets. *ACS Infectious Diseases*, **4**(5), 696 – 714. <https://doi.org/10.1021/acsinfecdis.7b00255>
- Wellington S, Nag PP, Michalska K, Johnston SE, Jedrzejczak RP, Kaushik VK, Clatworthy AE, Siddiqi N, McCarren P, Bajrami B, Maltseva NI. ...and Hung DT (2017).** A small-molecule allosteric inhibitor of *Mycobacterium tuberculosis* tryptophan synthase. *Nature Chemical Biology*, **13**(9), 943 – 950. <https://doi.org/10.1038/nchembio.2420>
- Yelamanchi SD and Surolia A (2021).** Targeting amino acid metabolism of *Mycobacterium tuberculosis* for developing inhibitors to curtail its survival. *IUBMB Life*, **73**(4), 643 – 58. <https://doi.org/10.1002/iub.2455>

Copyright: © 2025 by the Authors, published by Centre for Info Bio Technology. This article is an open access article distributed under the terms and conditions of the Creative Commons Attribution (CC BY-NC) license [<https://creativecommons.org/licenses/by-nc/4.0/>], which permit unrestricted use, distribution, and reproduction in any medium, for non-commercial purpose, provided the original work is properly cited.